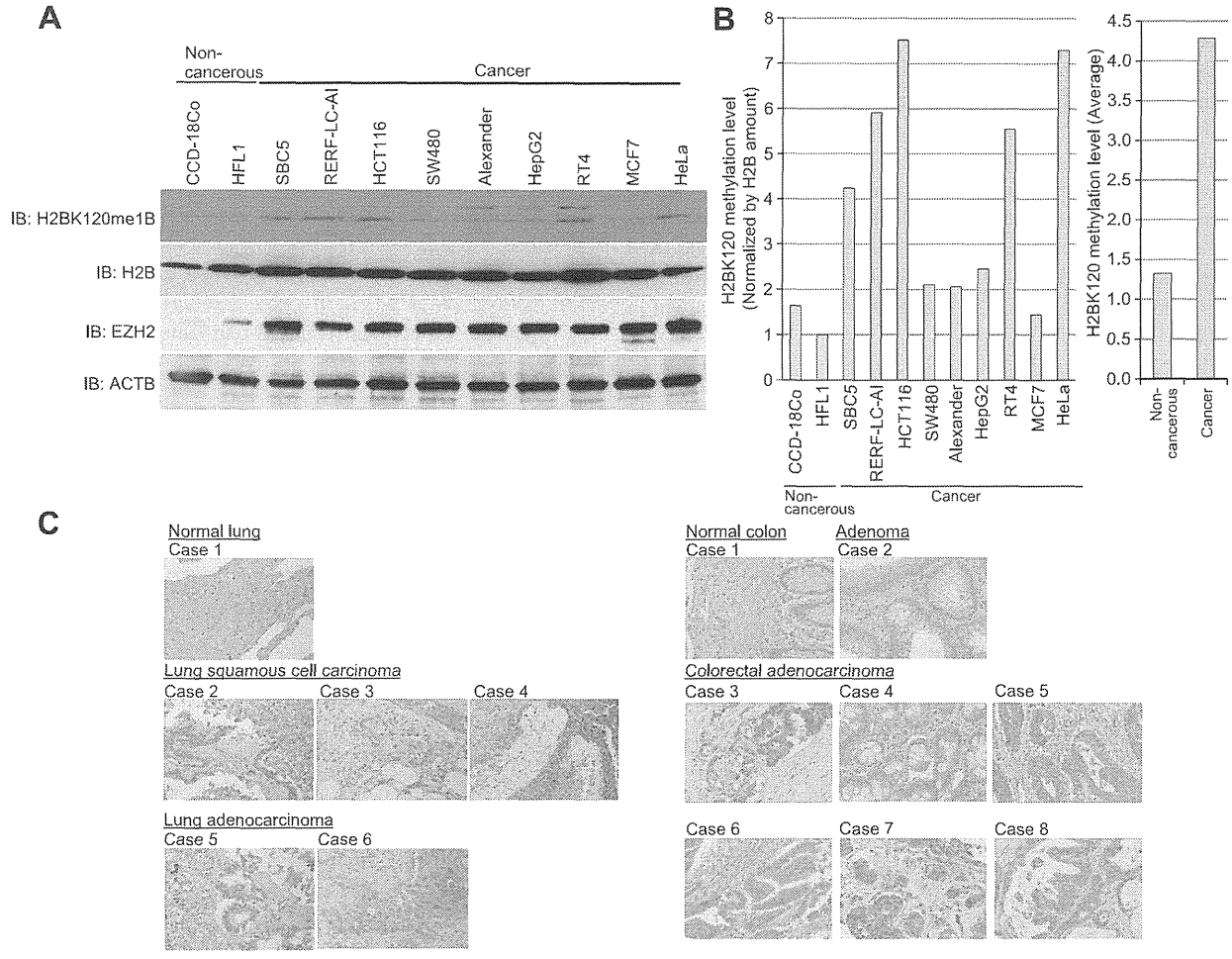

Figure 2. H2BK120 methylation is increased in cancer cells. (A) Validation of H2BK120 methylation status in various cell lines. Lysates from noncancerous cell lines (CCD-18Co and HFL1) and cancer cell lines (SBC5, RERF-LC-AI, HCT116, SW480, Alexander, HepG2, RT4, MCF7, and HeLa) were immunoblotted with anti-monomethylated K120 H2B, anti–histone H2B (ab1790; Abcam), anti-EZH2 (NCL-L-EZH2; Leica), and anti-ACTB (No. 4967; Cell Signaling Technology) antibodies. Information of certificated cell lines is described in Table W4. (B) Quantitative analysis of H2BK120 methylation levels. X-ray films were scanned with GS-800 calibrated densitometer (Bio-Rad Laboratories). The intensity of each H2BK120 monomethylation signal was normalized by the corresponding H2B signal and averaged. (C) Tissue microarray images of lung and colon tissues stained by standard immunohistochemistry for the methylation status of H2BK120. Clinical information for each section is represented in Tables W1 and W2. All tissue samples were purchased from BioChain (Newark, CA). Original magnification, ×200.

analysis to define the methylation site on H2B and found that H2BK120 was monomethylated by EZH2 (Figure 1*B*). We then generated anti–H2BK120-methylated antibodies using an H2BK120-methylated peptide (Figure W2). Among four different lots of the antibodies we obtained, we confirmed by slot blot analysis that H2BK120me1B showed the best quality of the result (Figure W3). In addition, ELISA analysis using this H2BK120-methylation–specific antibody clearly indicated that this antibody recognized the K120-methylated peptide but did not react to the unmethylated peptide, supporting the high specificity of this antibody against H2BK120 methylation (Figure 1*C*). To further verify the quality of the H2BK120-methylation antibody, we prepared both wild-type H2B (H2B-WT) and K120-substituted H2B (H2B-K120A) recombinant proteins and performed *in vitro* methyltransferase assays using EZH2. The H2BK120-methylation signal was increased in a dose-dependent manner, and the signal was completely diminished when H2B-K120A protein was used as a substrate (Figure 1*D*). Using the methylation-specific antibody, we performed immunocytochemical analysis after transfection of EZH2 vectors into HeLa cells to confirm EZH2-dependent H2BK120 methylation *in vivo* and detected the strong staining of methylated H2BK120 in EZH2-overexpressing cells (Figure 1*E*). Taken together, EZH2 can methylate H2BK120, and this methylation is also observed *in vivo*.

H2BK120 Monomethylation Is Increased in Cancer Cells

Because we previously found that the histone methyltransferase EZH2 was overexpressed in various types of cancer [1], we examined whether the methylation level of H2BK120 was enhanced in human cancer cells. Firstly, we prepared cell extracts of two noncancerous cell lines (CCD-18Co and HFL1) and nine cancer cell lines (SBC5, RERF-LC-AI, HCT116, SW480, Alexander, HepG2, RT4, MCF7,

and HeLa; Table W5), and conducted Western blot analysis using the specific antibody (Figure 2*A*). As we expected, the methylation levels of H2BK120 in cancer cell lines expressing high levels of EZH2 were higher than in noncancerous cell lines in which EZH2 expression was very low (Figures 2*B* and W4). We subsequently conducted immunohistochemical analysis of lung and colon tissues (one normal lung, three lung squamous cell carcinomas, and two lung adenocarcinomas as well as one normal colon, one colon adenoma, and six colorectal adenocarcinomas) using the methylation-specific antibody and found higher methylation levels of H2BK120 in cancer cells than normal cells (Figure 2*C*, *left* for lung and *right* for colon).

H2BK120 Monomethylation Competitively Inhibits Monoubiquitination

As H2BK120 was shown to be monoubiquitinated and play a crucial role in the transcriptional regulation, we examined the relationship between H2BK120 methylation and ubiquitination [9]. Immunocytochemial analysis was conducted after FLAG-tagged EZH2 expression vectors were transfected into HeLa cells. EZH2-transfected cells showed significantly lower signals of H2BK120 ubiquitination than control cells (Figure 3*A*). This result indicated that EZH2-dependent H2BK120 methylation appears to competitively inhibit the ubiquitination. In addition, we knocked down the expression of EZH2 in SBC5 cells and conducted the Western blot analysis using purified histone samples to validate the relationship between H2BK120 methylation and ubiquitination. Consistently, H2BK120 methylation status of purified histone H2B proteins was increased after knockdown of EZH2 (Figure 3*B*). Furthermore, we examined the status of H2BK120 ubiquitination in normal and cancer cells and confirmed that ubiquitination levels in cancer cells were lower than those in noncancerous cells (Figure W5). These results reveal that the histone methyltransferase EZH2 is likely to inhibit the

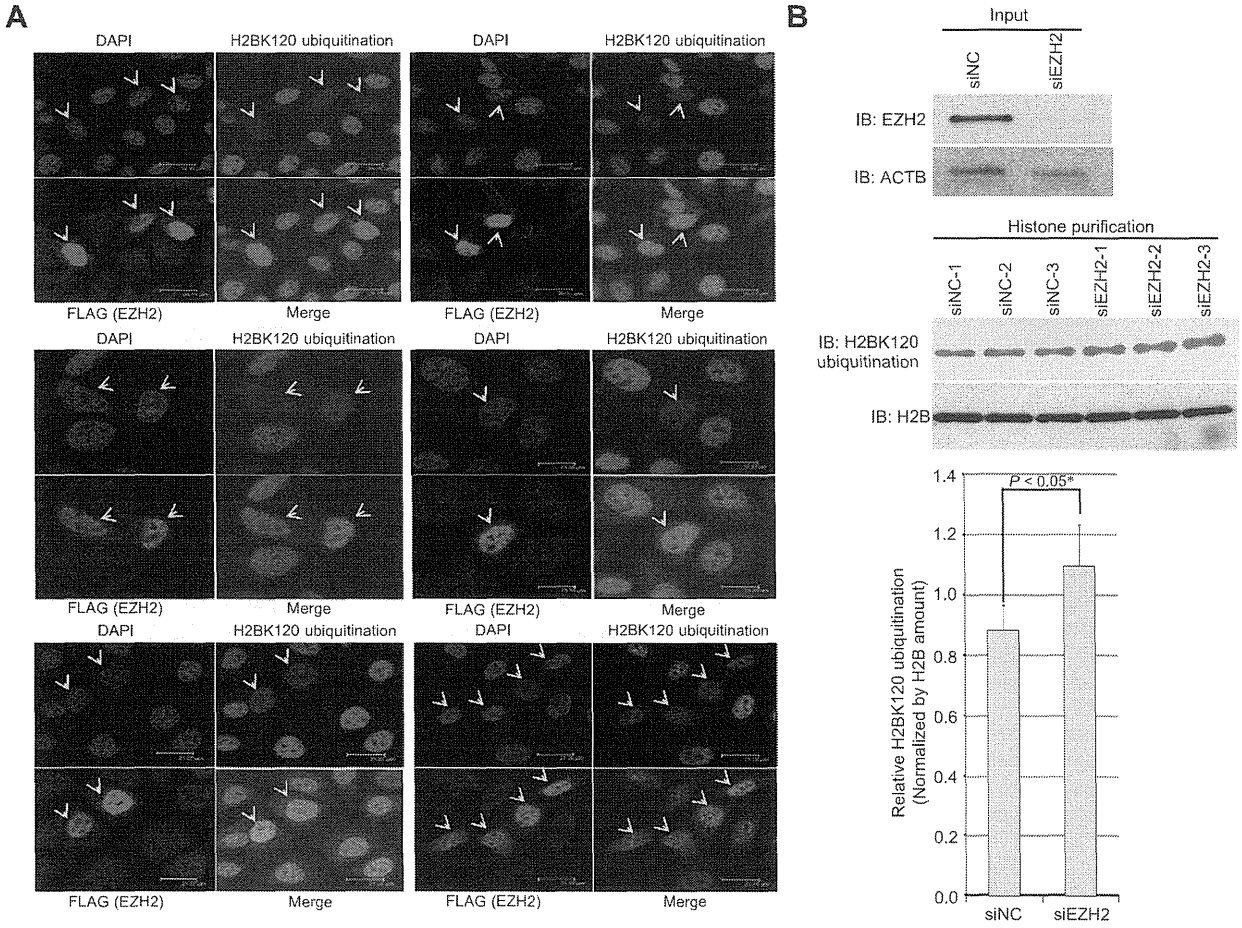

Figure 3. H2BK120 methylation competitively inhibited the ubiquitination. (A) Immunocytochemical analysis of HeLa cells. Cells were stained with an anti–Ubiquityl-Histone H2BK120 antibody (No. 5546; Cell Signaling Technology), an anti-FLAG antibody (M2; Sigma-Aldrich), and 4′,6′-diamidine-2′-phenylindole dihydrochloride [DAPI (blue)]. Alexa Fluor 488 (green) and Alexa Fluor 594 (red) antibodies were used as secondary antibodies. HeLa cells were fixed in 4% paraformaldehyde 24 hours after transfection of FLAG-tagged EZH2 expression vectors. (B) Effects of EZH2 knockdown on the ubiquitination of H2BK120 in SBC5 cells. SBC5 cells were lysed 48 hours after treatment with siNC and siEZH2. Samples were immunoblotted with anti-EZH2 (NCL-L-EZH2; Leica, upper) and anti–Ubiquityl-Histone H2BK120 (middle) antibodies. Expressions of ACTB (No. 4967; Cell Signaling Technology) and H2B (ab1790; Abcam) were the internal controls. The ubiquitination level of H2BK120 was calculated by GS-800 (Bio-Rad Laboratories, lower). Results are the means ± SD of three independent experiments. The *P* value was calculated using Student's *t* test.

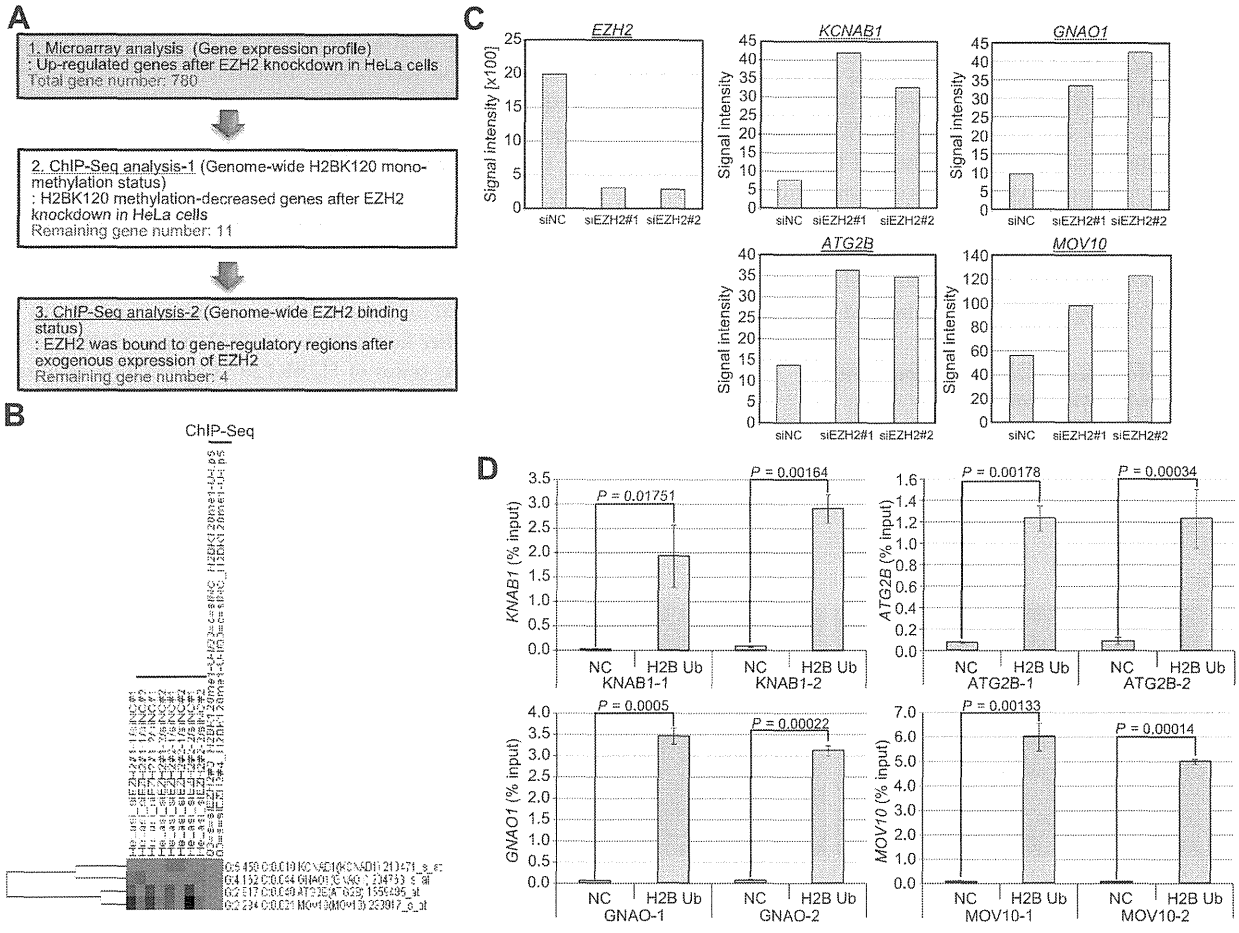

Figure 4. Direct downstream genes of EZH2 through the methylation of H2BK120. (A) Schematic diagram of the strategy to identify direct downstream genes of EZH2. Detailed procedures of ChIP-Seq and microarray analyses were described in Materials and Methods section. 1) Gene expression profile analysis was conducted using the Affymetrix GeneChip system after knockdown of EZH2 in HeLa cells. Seven hundred eighty genes were identified to be downregulated by EZH2 knockdown (>2.0). 2) Chip-Seq analysis to examine the methylation status of histone H2BK120 monomethylation in gene-regulatory regions. Among 780 genes identified by microarray analysis, the methylation status was decreased in 11 genes. 3) ChIP-Seq analysis to identify binding regions of EZH2 proteins after exogenous expression of EZH2. Finally, four genes remained as direct downstream genes of EZH2 through the methylation of H2BK120. (B) The heatmap of four genes directly regulated by EZH2 through the inhibition of histone H2BK120 methylation. Affymetrix GeneChip data (microarray analysis) and ChIP-Seq data were combined. G, the expression ratio of each target gene between siEZH2-treated and control cells (siEZH2/Control). C, the ratio of methylation status in the regulatory region of each gene (siEZH2/Control). Probe Set ID (HG-U133_Plus_2.na33.annotation) is shown with gene symbol. (C) Expression levels of *EZH2*, *KCNAB1*, *GNAO1*, *ATG2B*, and *MOV10* in HeLa cells were analyzed by Affymetrix GeneChip system. (D) ChIP analysis using primer pairs of downstream candidate genes as described under Materials and Methods section. Cross-linked and sheared chromatin was immunoprecipitated with an anti–Ubiquityl-Histone H2BK120 antibody (No. 5546; Cell Signaling Technology). Protein A Agarose/Salmon Sperm DNA (Millipore) was used as a negative control. Results are the means ± SD of three independent experiments and shown as a percentage of the input chromatin. The *P* value was calculated using Student's *t* test.

ubiquitination of H2BK120 in a competitive manner through the methylation of the lysine residue.

Mechanisms in Transcriptional Regulation through EZH2-Dependent H2BK120 Methylation

As it is known that H2BK120 ubiquitination plays a crucial role in the transcriptional regulation, we next examined the transcriptional regulation mechanism of EZH2-dependent H2BK120 methylation in cancer cells. To identify direct downstream genes of EZH2 through the methylation of H2BK120, we conducted cDNA microarray and ChIP-Seq analyses and combined the data. At first, cDNA microarray analysis using the Affymetrix GeneChip system was performed, and expression levels of 780 genes were increased after treatment with siEZH2 in HeLa cells (Figure 4*A*, more than two times compared with control). Then, we planned to do ChIP-Seq analysis to examine the genome-wide H2BK120 monomethylation status. Firstly, we validated the quality of the antibody whether it is available for immunoprecipitation or not. FLAG-conjugated wild-type H2B (H2B-WT) and K120-substituted H2B (H2B-K120A) expression vectors were

transfected into 293T cells, and cell lysates were immunoprecipitated with anti-H2BK120 methylation antibodies, followed by Western blot analysis using an anti-FLAG antibody (Figure W6*A*). Among three lots of anti-H2BK120 methylation antibodies, H2BK120me1B showed the best quality as well as slot blot analysis. To evaluate the availability of this antibody for the immunoprecipitation of endogenous H2BK1200-methylated proteins, Western blot analysis using the H2BK120me1B antibody was performed after immunoprecipitation of SBC5 cell lysates using the same antibody (Figure W6*B*). Subsequently, we confirmed the specific signal of K120-methylated H2B proteins, implying that this antibody is also available for the immunoprecipitation of endogenous K120-methylated histone H2B. On the basis of this result, ChIP-Seq analysis was conducted after treatment with siNC (negative control) and two independent siEZH2s, and among 780 genes selected by microarray analysis, the methylation status of gene-regulatory regions of 11 genes was significantly decreased (Figure 4*A*). In addition, we also examined the genome-wide EZH2-binding status to identify the gene-regulatory regions that EZH2 was bound by ChIP-Seq analysis. Finally, four genes (*KCNAB1*, *GNAO1*, *ATG2B*, and *MOV10*) remained as direct downstream genes of EZH2 through the methylation of H2BK120 after combining the data of microarray and ChIP-Seq analyses (Figure 4*B*). Detailed expression profile data of the four genes were shown in Figure 4*C*. These results reveal that EZH2-dependent H2BK120 methylation can regulate the transcription of downstream genes, and it is a novel mechanism of human carcinogenesis mediated by EZH2 overexpression.

Discussion

Histone H2B is a core histone, and so far, acetylation, phosphorylation, ubiquitination, and sumoylation have already been reported as posttranslational modifications of this protein. In the present study, we identified that lysine 120 of histone H2B is methylated by EZH2 and that the methylation competitively inhibits the

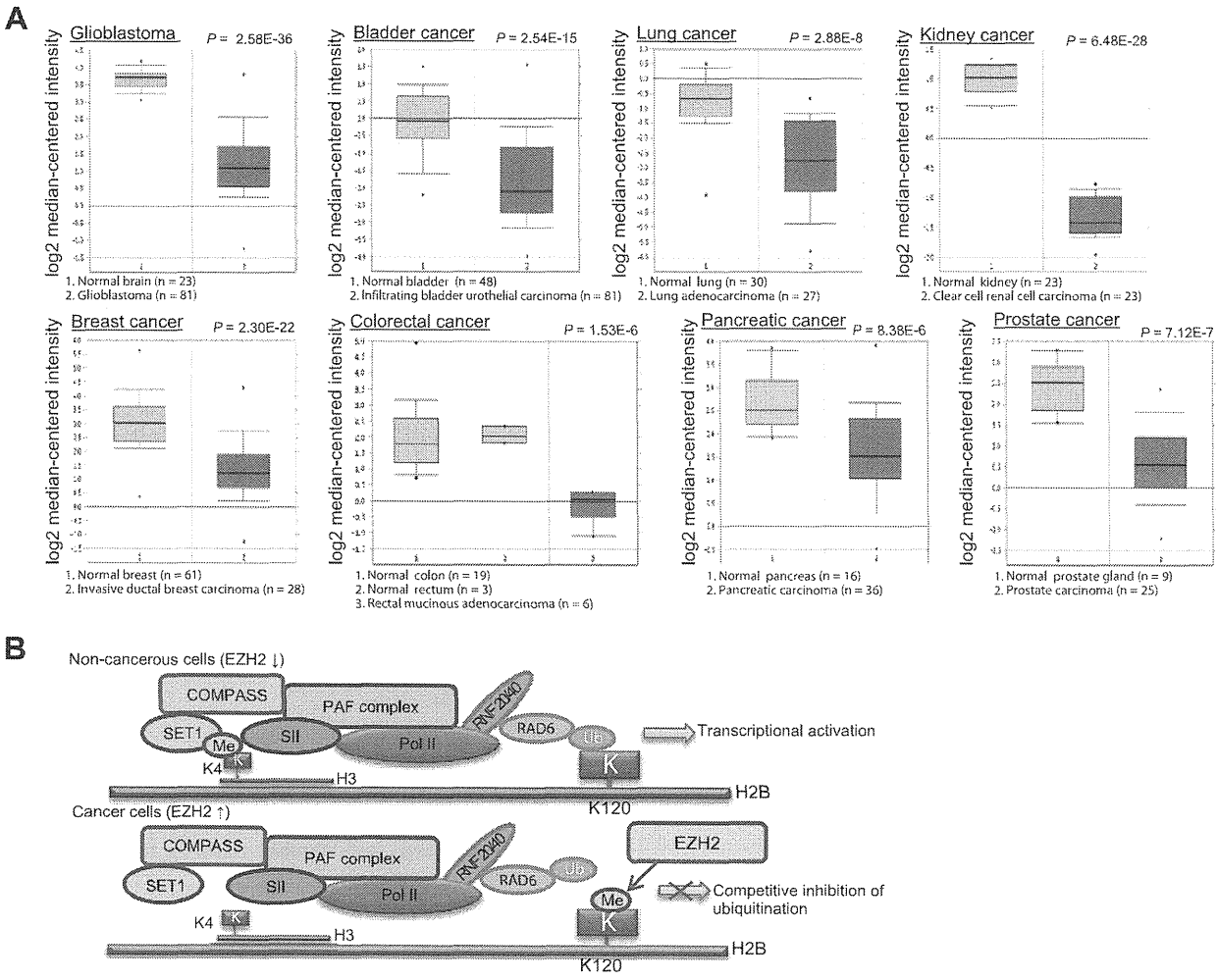

Figure 5. EZH2-dependent transcriptional regulation mechanism through H2BK120 methylation. (A) Expression of *KCNAB1* in cancer tissues. Expression levels of *KCNAB1* are downregulated in various types of cancer. Gene expression data in Oncomine (University of Michigan, Ann Arbor, MI) were analyzed. The thick bars in the boxes are average expression levels, and the boxes represent 95% of the samples. The error bars are above or below the boxes, and the range of expression levels is enclosed by two dots. (B) Proposed model for regulation of H2BK120 posttranslational modification during human carcinogenesis.

ubiquitination of H2BK120. This is the first report to describe the function of histone H2B methylation.

In mammals, H2BK120 monoubiquitination was reported to be preferentially associated with highly transcribed genes [10]. H2BK120 monoubiquitination can cooperate with facilitates chromatin transcription (FACT) and the polymerase associated factor (PAF) complex to regulate transcription elongation by RNA polymerase II [28] and can also facilitate DNA repair [29] and mRNA 3′ end processing [11] in human cells. In addition, Vitaliano-Prunier et al. recently reported that H2B ubiquitination in yeast cells plays a role in mRNA export from the nucleus into the cytoplasm [30]. Importantly, there are several reports describing the relationship between H2BK120 ubiquitination and cancer. The H2B deubiquitinase ubiquitin specific peptidase 22 (USP22) is part of a gene signature predictive of a cancer stem cell tumor phenotype of aggressive growth, metastasis, and therapy resistance [31]. RNF20, the E3 ubiquitin ligase for monoubiquitination of H2BK120, is a putative tumor suppressor [32]; its down-regulation in human cells promotes migration, anchorage independence, and carcinogenesis [32,33]. Furthermore, it was recently reported that H2B ubiquitination levels were decreased in advanced and metastatic breast cancer, parathyroid tumors, and seminoma [34–36]. These data imply that H2BK120 ubiquitination appears to possess tumor-suppressive functions, and its dysfunction causes malignant alteration of human cells.

In this study, we demonstrated that the histone methyltransferase EZH2 methylated H2BK120 and competitively inhibited the ubiquitination and that in cancer cells, the methylation level was increased, and the ubiquitination was decreased at lysine 120 of histone H2B. From these results, H2BK120 ubiquitination shows tumor-suppressive functions, and the oncogenic polycomb histone methyltransferase EZH2 competitively inhibits the ubiquitination through the methylation of H2BK120, which may result in the reduction of tumor-suppressive effects. In addition, we identified direct downstream genes of EZH2 through the methylation of H2BK120 on the basis of ChIP-Seq and microarray analyses (Figure 4*A*). Importantly, ChIP analysis indicated that H2BK120 ubiquitination levels of downstream candidate genes were significantly high in nontumor cells, implying that these genes may be transcriptionally activated in nontumor cells through the H2BK120 ubiquitination (Figure 4*D*). Among direct downstream candidates we identified, expression levels of *KCNAB1* and *GNAO1* are significantly decreased in various types of tumor tissues (Figures 5*A* and W7). *KCNAB1* is a voltage-gated potassium channel β subunit and modulates the activity of the pore-forming α subunit [37,38]. It has already been reported that some components of potassium channel serve as tumor suppressors. *KCTD11* (potassium channel tetramerization domain containing 11) is a novel tumor suppressor gene that inhibits cell growth and is mapping on human chromosome 17p13.2 [39]. According to the research using a panel of 177 human tumor samples and their normal matching samples representing 18 different types of cancer, down-regulation of KCTD11 protein level is a diffusely common event in tumorigenesis [40]. In addition, the putative tumor suppressor *KCNRG* (potassium channel–regulating gene) encodes a protein with a high homology to the tetramerization domain of voltage-gated K+ (Kv) channels [41]. This protein appears to interfere with the normal assembly of the K+ channel proteins by binding to their tetramerization domain, thereby causing the suppression of Kv currents [42]. Because Kv channels are involved in the proliferation of tumor cells [43] and normal lymphocytes [44], while being upregulated in neoplastic hematopoietic cells [45], *KCNRG* seems to exert a tumor suppressor effect [41]. On the contrary, *GNAO1*, a member of the signal-transducing guanine nucleotide-binding (G) protein family, has been implicated in ion channel regulation [46], and mutation of *GNAO1* was reported to cause the malignant alteration of cells [47,48]. *GPRC5a*, a family gene of *GNAO1*, is reported as a tumor suppressor gene, and knockout of GPCR5 leads to NF-κB activation in airway epithelium and promotes lung tumorigenesis [49]. Furthermore, according to expression profile analysis, expression levels of *ATG2B*, one of the autophagy-related genes, in several types of tumor tissues were much lower than those in corresponding normal tissues (Figure W8). Frameshift mutations of ATG2B were found in gastric and colorectal cancers [50]. The truncation mutants of ATG2B may inactivate its autophagy function and/or autophagic cell death, which resembles a typical loss-of-function mutation. These data imply that *KCNAB1*, *GNAO1*, and *ATG2B* are likely to be deregulated in cancer and work as tumor suppressors. Taken together, the oncogenic histone methyltransferase EZH2 is likely to contribute to human carcinogenesis based on the transcriptional regulation of downstream genes through not only H3K27 methylation but also H2BK120 methylation. In line with this, we also conducted the ChIP-Seq analysis and found that *GNAO1*, *ATG2B*, and *MOV10* were regulated by H2BK120 methylation, but the *KCNAB1* gene appears to be regulated by both H2BK120 methylation and H3K27 methylation (Table W6). This implies that some gene is likely to be synergistically regulated by two different histone marks.

All the while, histone H3-K27 has been only the known target of EZH2-dependent methylation, and the importance of EZH2 in human carcinogenesis was described only focusing on H3K27 methylation. In this study, we identified H2BK120 to be a novel target of EZH2-dependent methylation and downstream candidates through the novel methylation site (Figure 5*B*). Because EZH2 is overexpressed in various types of cancer and it plays a critical role in the growth regulation of cancer cells, EZH2 is recognized as an important target of anticancer treatment. In fact, chemical compounds, which inhibit methyltransferase activity of EZH2, have recently been developed as anticancer drugs. According to our findings, we need to take care of H2BK120 methylation besides H3K27 methylation to develop efficient anticancer treatment targeting EZH2, and the identification of this novel methylation site must contribute to unveil the multifunctions of EZH2 in human carcinogenesis. Furthermore, additional functional analysis of H2BK120 methylation may elucidate the significance of biologic function of this methylation, including disease like cancer, and the importance for diagnosis, prognosis, and treatment for cancer.

Acknowledgments

We thank Hyun-Soo Cho, Kzuyuki Hayashi, Kazuhiro Maejima, Yuka Yamane, Yukiko Iwai, and Haruka Sawada for technical assistance.

References

[1] Takawa M, Masuda K, Kunizaki M, Daigo Y, Takagi K, Iwai Y, Cho HS, Toyokawa G, Yamane Y, Maejima K, et al. (2011). Validation of the histone methyltransferase EZH2 as a therapeutic target for various types of human cancer and as a prognostic marker. *Cancer Sci* **102**, 1298–1305.

[2] Knutson SK, Wigle TJ, Warholic NM, Sneeringer CJ, Allain CJ, Klaus CR, Sacks JD, Raimondi A, Majer CR, Song J, et al. (2012). A selective inhibitor of EZH2 blocks H3K27 methylation and kills mutant lymphoma cells. *Nat Chem Biol* **8**, 890–896.

[3] McCabe MT, Ott HM, Ganji G, Korenchuk S, Thompson C, Van Aller GS, Liu Y, Graves AP, Della Pietra A III, Diaz E, et al. (2012). EZH2 inhibition as a therapeutic strategy for lymphoma with EZH2-activating mutations. *Nature* **492**, 108–112.

[4] Schiltz RL, Mizzen CA, Vassilev A, Cook RG, Allis CD, and Nakatani Y (1999). Overlapping but distinct patterns of histone acetylation by the human coactivators p300 and PCAF within nucleosomal substrates. *J Biol Chem* **274**, 1189–1192.

[5] Suka N, Suka Y, Carmen AA, Wu J, and Grunstein M (2001). Highly specific antibodies determine histone acetylation site usage in yeast heterochromatin and euchromatin. *Mol Cell* **8**, 473–479.

[6] Cheung WL, Ajiro K, Samejima K, Kloc M, Cheung P, Mizzen CA, Beeser A, Etkin LD, Chernoff J, Earnshaw WC, et al. (2003). Apoptotic phosphorylation of histone H2B is mediated by mammalian sterile twenty kinase. *Cell* **113**, 507–517.

[7] Zhu B, Zheng Y, Pham AD, Mandal SS, Erdjument-Bromage H, Tempst P, and Reinberg D (2005). Monoubiquitination of human histone H2B: the factors involved and their roles in *HOX* gene regulation. *Mol Cell* **20**, 601–611.

[8] Nathan D, Ingvarsdottir K, Sterner DE, Bylebyl GR, Dokmanovic M, Dorsey JA, Whelan KA, Krsmanovic M, Lane WS, Meluh PB, et al. (2006). Histone sumoylation is a negative regulator in *Saccharomyces cerevisiae* and shows dynamic interplay with positive-acting histone modifications. *Genes Dev* **20**, 966–976.

[9] Sun ZW and Allis CD (2002). Ubiquitination of histone H2B regulates H3 methylation and gene silencing in yeast. *Nature* **418**, 104–108.

[10] Minsky N, Shema E, Field Y, Schuster M, Segal E, and Oren M (2008). Monoubiquitinated H2B is associated with the transcribed region of highly expressed genes in human cells. *Nat Cell Biol* **10**, 483–488.

[11] Pirngruber J, Shchebet A, Schreiber L, Shema E, Minsky N, Chapman RD, Eick D, Aylon Y, Oren M, and Johnsen SA (2009). CDK9 directs H2B monoubiquitination and controls replication-dependent histone mRNA 3′-end processing. *EMBO Rep* **10**, 894–900.

[12] Kim J, Hake SB, and Roeder RG (2005). The human homolog of yeast BRE1 functions as a transcriptional coactivator through direct activator interactions. *Mol Cell* **20**, 759–770.

[13] Fierz B, Chatterjee C, McGinty RK, Bar-Dagan M, Raleigh DP, and Muir TW (2011). Histone H2B ubiquitylation disrupts local and higher-order chromatin compaction. *Nat Chem Biol* **7**, 113–119.

[14] Fuchs G, Shema E, Vesterman R, Kotler E, Wolchinsky Z, Wilder S, Golomb L, Pribluda A, Zhang F, Haj-Yahya M, et al. (2012). RNF20 and USP44 regulate stem cell differentiation by modulating H2B monoubiquitylation. *Mol Cell* **46**, 662–673.

[15] Hamamoto R, Furukawa Y, Morita M, Iimura Y, Silva FP, Li M, Yagyu R, and Nakamura Y (2004). *SMYD3* encodes a histone methyltransferase involved in the proliferation of cancer cells. *Nat Cell Biol* **6**, 731–740.

[16] Hamamoto R, Silva FP, Tsuge M, Nishidate T, Katagiri T, Nakamura Y, and Furukawa Y (2006). Enhanced SMYD3 expression is essential for the growth of breast cancer cells. *Cancer Sci* **97**, 113–118.

[17] Cho HS, Shimazu T, Toyokawa G, Daigo Y, Maehara Y, Hayami S, Ito A, Masuda K, Ikawa N, Field HI, et al. (2012). Enhanced HSP70 lysine methylation promotes proliferation of cancer cells through activation of Aurora kinase B. *Nat Commun* **3**, 1072.

[18] Cho HS, Suzuki T, Dohmae N, Hayami S, Unoki M, Yoshimatsu M, Toyokawa G, Takawa M, Chen T, Kurash JK, et al. (2011). Demethylation of RB regulator MYPT1 by histone demethylase LSD1 promotes cell cycle progression in cancer cells. *Cancer Res* **71**, 655–660.

[19] Takawa M, Cho HS, Hayami S, Toyokawa G, Kogure M, Yamane Y, Iwai Y, Maejima K, Ueda K, Masuda A, et al. (2012). Histone lysine methyltransferase SETD8 promotes carcinogenesis by deregulating PCNA expression. *Cancer Res* **72**, 3217–3227.

[20] Hayami S, Kelly JD, Cho HS, Yoshimatsu M, Unoki M, Tsunoda T, Field HI, Neal DE, Yamaue H, Ponder BA, et al. (2011). Overexpression of LSD1 contributes to human carcinogenesis through chromatin regulation in various cancers. *Int J Cancer* **128**, 574–586.

[21] Kogure M, Takawa M, Cho HS, Toyokawa G, Hayashi K, Tsunoda T, Kobayashi T, Daigo Y, Sugiyama M, Atomi Y, et al. (2013). Deregulation of the histone demethylase JMJD2A is involved in human carcinogenesis through regulation of the G_1/S transition. *Cancer Lett* **336**, 76–84.

[22] Li H and Durbin R (2009). Fast and accurate short read alignment with Burrows–Wheeler transform. *Bioinformatics* **25**, 1754–1760.

[23] Zhang Y, Liu T, Meyer CA, Eeckhoute J, Johnson DS, Bernstein BE, Nusbaum C, Myers RM, Brown M, Li W, et al. (2008). Model-based analysis of ChIP-Seq (MACS). *Genome Biol* **9**, R137.

[24] Feng J, Liu T, and Zhang Y (2011). Using MACS to identify peaks from ChIP-Seq data. *Curr Protoc Bioinformatics* **34**, 2.14.1–2.14.14. Chapter 2, Unit 2 14.

[25] Kadota K, Nishiyama T, and Shimizu K (2012). A normalization strategy for comparing tag count data. *Algorithms Mol Biol* **7**, 5.

[26] Hayami S, Yoshimatsu M, Veerakumarasivam A, Unoki M, Iwai Y, Tsunoda T, Field HI, Kelly JD, Neal DE, Yamaue H, et al. (2010). Overexpression of the JmjC histone demethylase KDM5B in human carcinogenesis: involvement in the proliferation of cancer cells through the E2F/RB pathway. *Mol Cancer* **9**, 59.

[27] Yoshimatsu M, Toyokawa G, Hayami S, Unoki M, Tsunoda T, Field HI, Kelly JD, Neal DE, Maehara Y, Ponder BA, et al. (2011). Dysregulation of PRMT1 and PRMT6, type I arginine methyltransferases, is involved in various types of human cancers. *Int J Cancer* **128**, 562–573.

[28] Pavri R, Zhu B, Li G, Trojer P, Mandal S, Shilatifard A, and Reinberg D (2006). Histone H2B monoubiquitination functions cooperatively with FACT to regulate elongation by RNA polymerase II. *Cell* **125**, 703–717.

[29] Moyal L, Lerenthal Y, Gana-Weisz M, Mass G, So S, Wang SY, Eppink B, Chung YM, Shalev G, Shema E, et al. (2011). Requirement of ATM-dependent monoubiquitylation of histone H2B for timely repair of DNA double-strand breaks. *Mol Cell* **41**, 529–542.

[30] Vitaliano-Prunier A, Babour A, Hérissant L, Apponi L, Margaritis T, Holstege FC, Corbett AH, Gwizdek C, and Dargemont C (2012). H2B ubiquitylation controls the formation of export-competent mRNP. *Mol Cell* **45**, 132–139.

[31] Zhang XY, Varthi M, Sykes SM, Phillips C, Warzecha C, Zhu W, Wyce A, Thorne AW, Berger SL, and McMahon SB (2008). The putative cancer stem cell marker USP22 is a subunit of the human SAGA complex required for activated transcription and cell-cycle progression. *Mol Cell* **29**, 102–111.

[32] Shema E, Tirosh I, Aylon Y, Huang J, Ye C, Moskovits N, Raver-Shapira N, Minsky N, Pirngruber J, Tarcic G, et al. (2008). The histone H2B-specific ubiquitin ligase RNF20/hBRE1 acts as a putative tumor suppressor through selective regulation of gene expression. *Genes Dev* **22**, 2664–2676.

[33] Shema E, Kim J, Roeder RG, and Oren M (2011). RNF20 inhibits TFIIS-facilitated transcriptional elongation to suppress pro-oncogenic gene expression. *Mol Cell* **42**, 477–488.

[34] Chernikova SB, Razorenova OV, Higgins JP, Sishc BJ, Nicolau M, Dorth JA, Chernikova DA, Kwok S, Brooks JD, Bailey SM, et al. (2012). Deficiency in mammalian histone H2B ubiquitin ligase Bre1 (Rnf20/Rnf40) leads to replication stress and chromosomal instability. *Cancer Res* **72**, 2111–2119.

[35] Hahn MA, Dickson KA, Jackson S, Clarkson A, Gill AJ, and Marsh DJ (2012). The tumor suppressor CDC73 interacts with the ring finger proteins RNF20 and RNF40 and is required for the maintenance of histone 2B monoubiquitination. *Hum Mol Genet* **21**, 559–568.

[36] Prenzel T, Begus-Nahrmann Y, Kramer F, Hennion M, Hsu C, Gorsler T, Hintermair C, Eick D, Kremmer E, Simons M, et al. (2011). Estrogen-dependent gene transcription in human breast cancer cells relies upon proteasome-dependent monoubiquitination of histone H2B. *Cancer Res* **71**, 5739–5753.

[37] Leicher T, Roeper J, Weber K, Wang X, and Pongs O (1996). Structural and functional characterization of human potassium channel subunit β1 (KCNA1B). *Neuropharmacology* **35**, 787–795.

[38] Schultz D, Litt M, Smith L, Thayer M, and McCormack K (1996). Localization of two potassium channel β subunit genes, KCNA1B and KCNA2B. *Genomics* **31**, 389–391.

[39] Di Marcotullio L, Ferretti E, De Smaele E, Argenti B, Mincione C, Zazzeroni F, Gallo R, Masuelli L, Napolitano M, Maroder M, et al. (2004). REN^{KCTD11} is a suppressor of Hedgehog signaling and is deleted in human medulloblastoma. *Proc Natl Acad Sci USA* **101**, 10833–10838.

[40] Mancarelli MM, Zazzeroni F, Ciccocioppo L, Capece D, Po A, Murgo S, Di Camillo R, Rinaldi C, Ferretti E, Gulino A, et al. (2010). The tumor suppressor gene $KCTD11^{REN}$ is regulated by Sp1 and methylation and its expression is reduced in tumors. *Mol Cancer* **9**, 172.

[41] Birerdinc A, Nohelty E, Marakhonov A, Manyam G, Panov I, Coon S, Nikitin E, Skoblov M, Chandhoke V, and Baranova A (2010). Pro-apoptotic and anti-proliferative activity of human *KCNRG*, a putative tumor suppressor in 13q14 region. *Tumour Biol* **31**, 33–45.

[42] Ivanov DV, Tyazhelova TV, Lemonnier L, Kononenko N, Pestova AA, Nikitin EA, Prevarskaya N, Skryma R, Panchin YV, Yankovsky NK, et al. (2003).

A new human gene *KCNRG* encoding potassium channel regulating protein is a cancer suppressor gene candidate located in 13q14.3. *FEBS Lett* **539**, 156–160.

[43] Rybalchenko V, Prevarskaya N, Van Coppenolle F, Legrand G, Lemonnier L, Le Bourhis X, and Skryma R (2001). Verapamil inhibits proliferation of LNCaP human prostate cancer cells influencing K+ channel gating. *Mol Pharmacol* **59**, 1376–1387.

[44] Lewis RS and Cahalan MD (1995). Potassium and calcium channels in lymphocytes. *Annu Rev Immunol* **13**, 623–653.

[45] Smith BC and Denu JM (2009). Chemical mechanisms of histone lysine and arginine modifications. *Biochim Biophys Acta* **1789**, 45–57.

[46] Murtagh JJ Jr, Eddy R, Shows TB, Moss J, and Vaughan M (1991). Different forms of Go alpha mRNA arise by alternative splicing of transcripts from a single gene on human chromosome 16. *Mol Cell Biol* **11**, 1146–1155.

[47] Garcia-Marcos M, Ghosh P, and Farquhar MG (2011). Molecular basis of a novel oncogenic mutation in GNAO1. *Oncogene* **30**, 2691–2696.

[48] Kan Z, Jaiswal BS, Stinson J, Janakiraman V, Bhatt D, Stern HM, Yue P, Haverty PM, Bourgon R, Zheng J, et al. (2010). Diverse somatic mutation patterns and pathway alterations in human cancers. *Nature* **466**, 869–873.

[49] Deng J, Fujimoto J, Ye XF, Men TY, Van Pelt CS, Chen YL, Lin XF, Kadara H, Tao Q, Lotan D, et al. (2010). Knockout of the tumor suppressor gene *Gprc5a* in mice leads to NF-κB activation in airway epithelium and promotes lung inflammation and tumorigenesis. *Cancer Prev Res (Phila)* **3**, 424–437.

[50] Kang MR, Kim MS, Oh JE, Kim YR, Song SY, Kim SS, Ahn CH, Yoo NJ, and Lee SH (2009). Frameshift mutations of autophagy-related genes *ATG2B*, *ATG5*, *ATG9B* and *ATG12* in gastric and colorectal cancers with microsatellite instability. *J Pathol* **217**, 702–706.

Table W1. Characteristics of Lung Tissues.

Case No.	Age	Gender	Pathology	Grade	Stage (TNM)	Nature
Case 1	34	Male	Normal	Normal		
Case 2	58	Male	Squamous cell carcinoma	II	T2N0M0	Malignant
Case 3	42	Male	Squamous cell carcinoma	II	T2N0M0	Malignant
Case 4	57	Male	Squamous cell carcinoma	III	T2N0M0	Malignant
Case 5	62	Male	Adenocarcinoma	II	T2N0M0	Malignant
Case 6	73	Male	Adenosquamous carcinoma	III	T2N1M0	Malignant

Table W2. Characteristics of Colon Tissues.

Case No.	Age	Gender	Histology	Grade	Stage (TNM)	Anatomic Site
Case 1	49	Female	Normal			Colon
Case 2	65	Male	Adenoma			Colon
Case 3	51	Male	Adenocarcinoma	II	T3N1M0	Colon
Case 4	39	Female	Adenocarcinoma	I_II	T3N1M0	Colon
Case 5	49	Female	Adenocarcinoma	I_II	T3N0M0	Colon
Case 6	62	Female	Adenocarcinoma	I_II	T2N1M0	Colon
Case 7	60	Male	Adenocarcinoma	II	T2N1M0	Colon
Case 8	34	Male	Adenocarcinoma	I	T3N0M0	Colon

Table W3. siRNA Sequences.

siRNA Name	Sequence
siNC (cocktail)	
Target No. 1	Sense: 5′ AUCCGCGCGAUAGUACGUA3′
	Antisense: 5′ UACGUACUAUCGCGCGGAU 3′
Target No. 2	Sense: 5′ UUACGCGUAGCGUAAUACG 3′
	Antisense: 5′ CGUAUUACGCUACGCGUAA 3′
Target No. 3	Sense: 5′ UAUUCGCGCGUAUAGCGGU 3′
	Antisense: 5′ ACCGCUAUACGCGCGAAUA 3′
siEZH2 No. 1	Sense: 5′ CUAACCAUGUUUACAACUA 3′
	Antisense: 5′ UAGUUGUAAACAUGGUUAG 3′
siEZH2 No. 2	Sense: 5′ GACAGAAGAGGGAAAGUGU 3′
	Antisense: 5′ ACACUUUCCCUCUUCUGUC 3′

Table W4. Primer Sequences for ChIP Analysis.

Name	Sequence	Length	Tm (°C)	MW
KCNAB1 Set 1 (KCNAB1-1): Amplification Size = 123				
KCNAB1-ChIP-f1	TTC CGT GTT CGA AGA TAC CAC	21	59.5	6381.2
KCNAB1-ChIP-r1	AAC CTT ATC CTG CCA CAA AGC	21	59.5	6319.2
KCNAB1 Set 2 (KCNAB1-2): Amplification Size = 119				
KCNAB1-ChIP-f2	ATT TGT CAG AAG TGC TGG GAG G	22	62.1	6870.5
KCNAB1-ChIP-r2	TCT TTG AAT GTC AGT GAA CCA C	22	58.4	6709.4
GNAO1 Set 1 (GNAO1-1): Amplification Size = 139				
GNAO1-ChIP-f1	AGC CTC GGG TGT CAC ATA TTA G	22	62.1	6750.4
GNAO1-ChIP-r1	CTC AGG AAA CGC GAT GTG GTA G	22	64.2	6824.5
GNAO1 Set 2 (GNAO1-2): Amplification Size = 118				
GNAO1-ChIP-f2	ATT CCG ACC CAC TAC CAC ATC	21	61.2	6255.1
GNAO1-ChIP-r2	GGG CCG GCT CTC CAT CTT GTC	21	67.3	6365.2
ATG2B Set 1 (ATG2B-1): Amplification Size = 122				
ATG2B-ChIP-f1	TCG GAG CCG GAA CTG CTC CAG	21	67.3	6432.2
ATG2B-ChIP-r1	CTC CTG GCG CGT TCA CGA GAC	21	67.3	6383.2
ATG2B Set 2 (ATG2B-2): Amplification Size = 98				
ATG2B-ChIP-f2	CCA GGA TTA AGC GAG CGT ATG	21	61.2	6495.3
ATG2B-ChIP-r2	CCC CGC CTC ATT CAG GTA TTG	21	63.2	6333.2
MOV10 Set 1 (MOV10-1): Amplification Size = 149				
MOV10-ChIP-f1	TTC CCA CTG ACA TTG CAT TTC	21	57.5	6307.2
MOV10-ChIP-r1	AGG CCA CAC ACT CAA TCT ACG	21	61.2	6344.2
MOV10 Set 2 (MOV10-2): Amplification Size = 104				
MOV10-ChIP-f2	TTA CTG TGT ATC CTG GCA GAG C	22	62.1	6741.4
MOV10-ChIP-r2	CAT AAG GGT CAA AGA AGT TTG G	22	58.4	6847.6

Tm indicates melting temperature; MW, molecular weight.

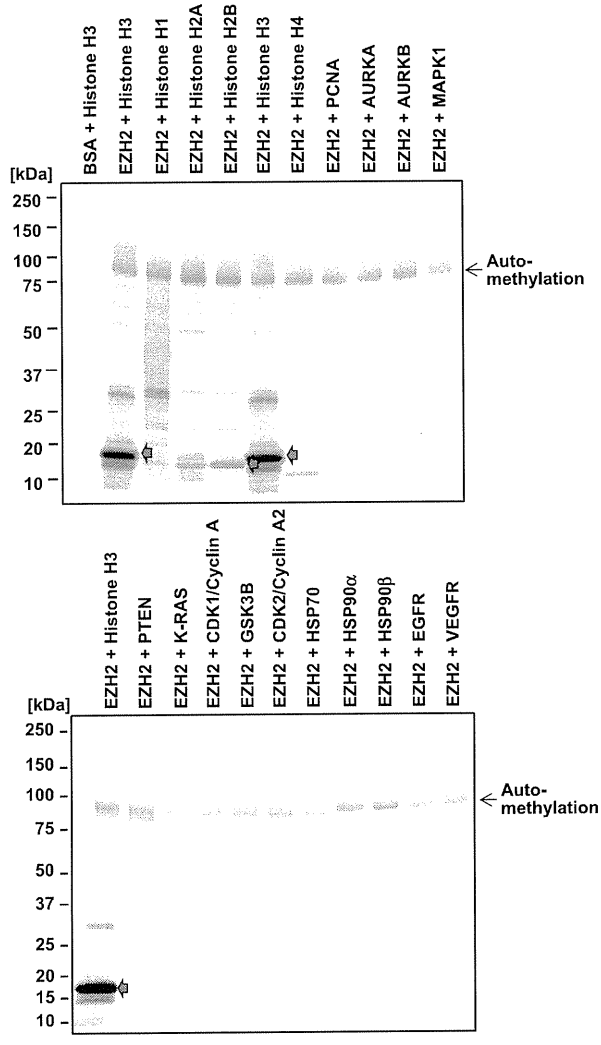

Figure W1. EZH2 methylates histone H2B. *In vitro* methyltransferase of EZH2 was performed using various types of recombinant proteins as substrates. Methylated proteins were visualized with fluorography.

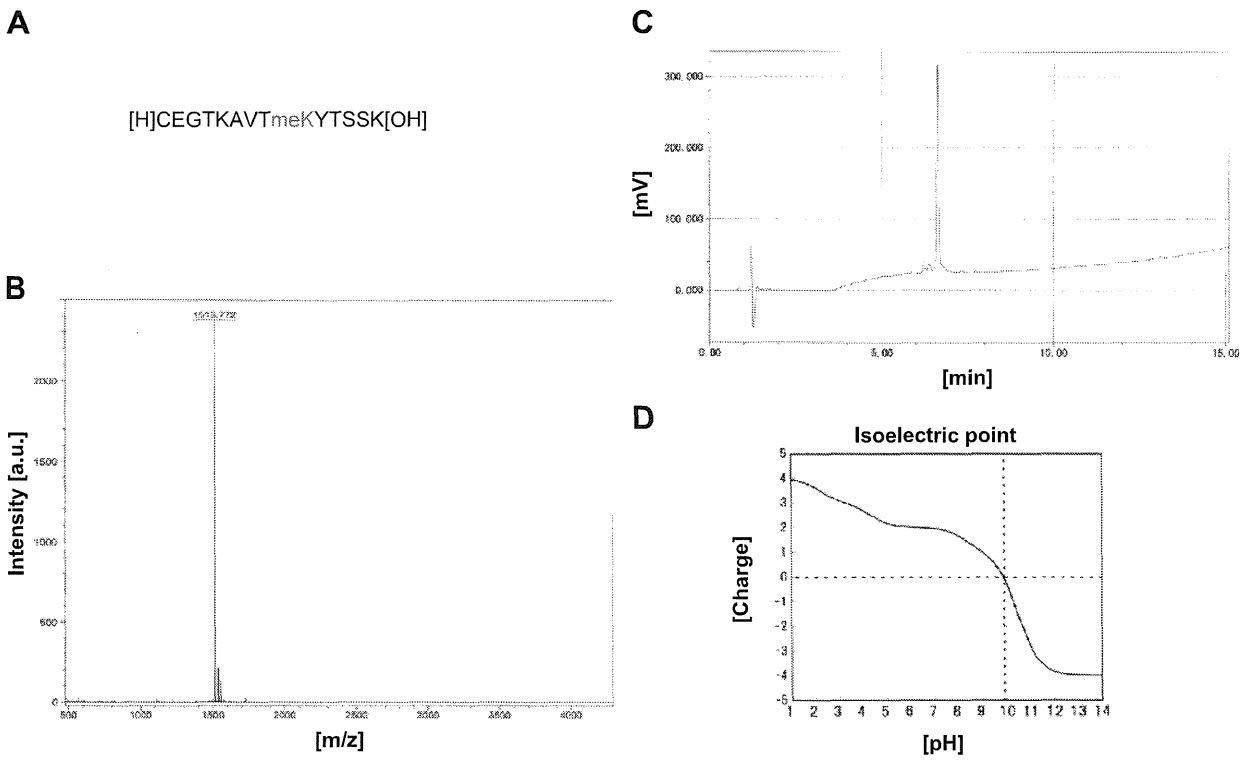

Figure W2. Quality check of peptides used as immunogens. (A) Amino acid sequence of the peptide. Ninth lysine residue is monomethylated. (B) Mass spectrum of the peptide. Bruker Daltonics flexAnalysis software (Billerica, MA) was used for the analysis. (C) Chromatogram of the peptide analyzed by the MultiStation LC-8020 system. (D) Isoelectric point figure of the peptide.

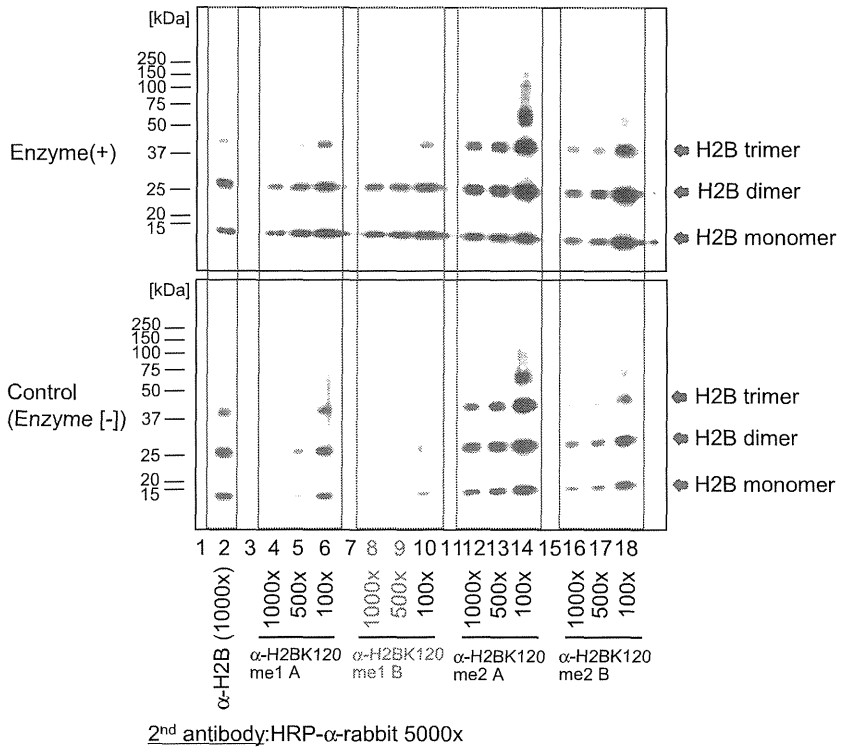

Figure W3. Slot blot analysis for the quality check of antibodies. *In vitro* methyltransferase assays were performed using recombinant EZH2 enzyme complex (No. 51004; BPS Bioscience) as an enzyme source. Samples were fractionated with SDS-PAGE and transferred to the nitrocellulose membranes. Slot blot analysis was conducted using anti-H2BK120 antibodies. An anti–histone H2B antibody was used as an internal control.

Table W5. Information of Certificated Cell Lines.

Name	Origin	Certification Institution	Tested Method	DNA Profile or Characteristics
CCD-18Co	human colonic fibroblast	ATCC	STR	Amelogenin: X CSF1PO: 8 D13S317: 12 D16S539: 12,13 D5S818: 12 D7S820: 8 THO1: 6,7 TPOX: 8,11 vWA: 15,17
HFL1	human fetal lung fibroblast	ATCC	STR	Amelogenin: X,Y CSF1PO: 10,12 D13S317: 11,12 D16S539: 9,11 D5S818: 12 D7S820: 9,10 THO1: 7,9 TPOX: 6,9 vWA: 17
SBC5	human small lung cancer	JCRB	STR	Amelogenin: X,Y TPOX: 9,12 CSF1PO: 10 D5S818: 10,11 D13S317: 8,10 D7S820: 8,11 D16S539: 12 vWA: 14,18 TH01: 6
RERF-LC-AI	human lung squamous cell carcinoma	JCRB	STR	Amelogenin: X,Y TPOX: 10,11 CSF1PO: 12 D5S818: 10.3 D13S317: 10 D7S820: 10,11 D16S539: 11 VWA: 17 TH01: 7,9
HCT116	human colorectal carcinoma	ATCC	STR	Amelogenin: X,Y CSF1PO: 7,10 D13S317: 10,12 D16S539: 11,13 D5S818: 10,11 D7S820: 11,12 THO1: 8,9 TPOX: 8,9 vWA: 17,22
SW480	human colorectal carcinoma	ATCC	STR	Amelogenin: X CSF1PO: 13,14 D13S317: 12 D16S539: 13 D5S818: 13 D7S820: 8 THO1: 8 TPOX: 11 vWA: 16
Alexander	human malignant liver cancer	JCRB	STR	D5S818: 12 D13S317: 11,12 D7S820: 9,11 D16S539: 13 vWA: 15,16 TH01: 7,8 Amelogenin: X TPOX: 8 CSF1PO: 10
RT4	human urinary bladder cancer	ATCC	STR	Amelogenin: X,Y CSF1PO: 10,12 D13S317: 8 D16S539: 9 D5S818: 11,12 D7S820: 9,12 THO1: 9,9.3 TPOX: 8,11 vWA: 14,17
MCF7	human breast adenocarcinoma	ATCC	STR	Amelogenin: X CSF1PO: 10 D13S317: 11 D16S539: 11,12 D5S818: 11,12 D7S820: 8.9 THO1: 6 TPOX: 9,12 vWA: 14,15
HeLa	human cervix carcinoma	ATCC	STR	Amelogenin: X,Y CSF1PO: 11,12 D13S317: 11,14 D16S539: 9,11 D5S818: 11,12 D7S820: 10,11 THO1: 8 TPOX: 8 vWA: 15

ATCC indicates American Type Culture Collection; JCRB, Japanese Collection of Research Bioresources.

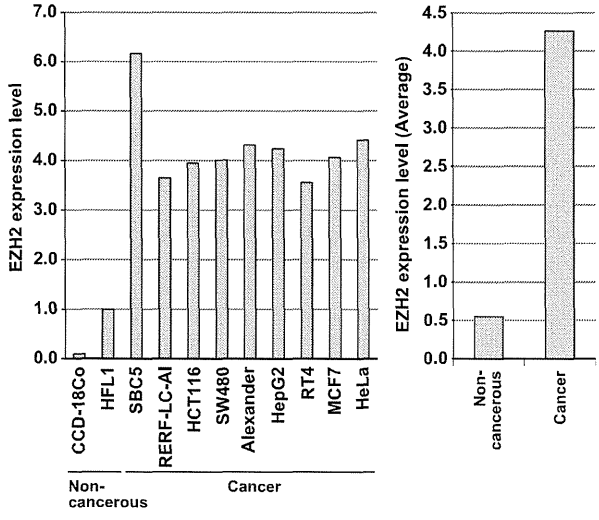

Figure W4. Quantitative analysis of EZH2 expression in various types of cell lines. X-ray films were scanned with GS-800 calibrated densitometer (Bio-Rad Laboratories). The intensity of each EZH2 signal was normalized by the corresponding ACTB signal and averaged.

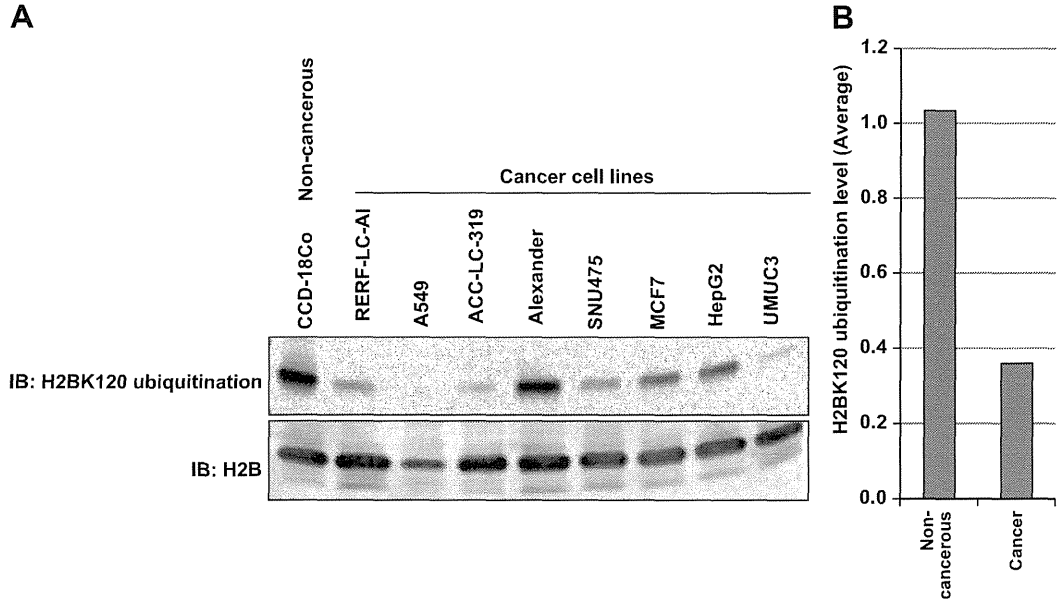

Figure W5. H2BK120 ubiquitination was decreased in cancer cells. (A) Validation of H2BK120 ubiquitination status in various cell lines. Lysates from a noncancerous cell line (CCD-18Co) and cancer cell lines (RERF-LC-AI, A549, ACC-LC-319, Alexander, SNU475, MCF7, HepG2, and UMUC3) were immunoblotted with anti–Ubiquityl-Histone H2BK120 antibody (No. 5546; Cell Signaling Technology) and anti–histone H2B (ab1790; Abcam) antibodies. (B) Quantitative analysis of H2BK120 ubiquitination levels. X-ray films were scanned with GS-800 calibrated densitometer (Bio-Rad Laboratories). The intensity of each H2BK120 ubiquitination signal was normalized by the corresponding H2B signal and averaged.

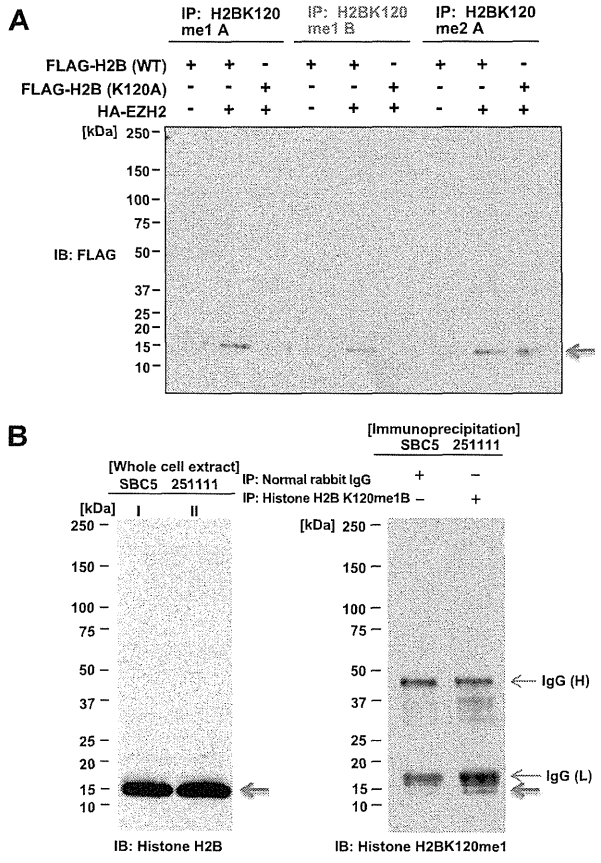

Figure W6. Validation of anti-H2BK120 methylation antibodies. (A) Wild-type FLAG-H2B (H2B-WT) and lysine 120–substituted FLAG-H2B expression vectors (K120A) were transfected into 293T cells. Cell lysates were immunoprecipitated with anti-H2BK120 methylation antibodies, and immunoblot analysis was performed using an anti-FLAG antibody (M2; Sigma-Aldrich). (B) SBC5 cells were lysed with CelLytic M, and cell lysates were immunoprecipitated with an anti-H2BK120 methylation antibody. Whole-cell extracts were blotted with an antihistone H2B antibody (Abcam; ab1790).

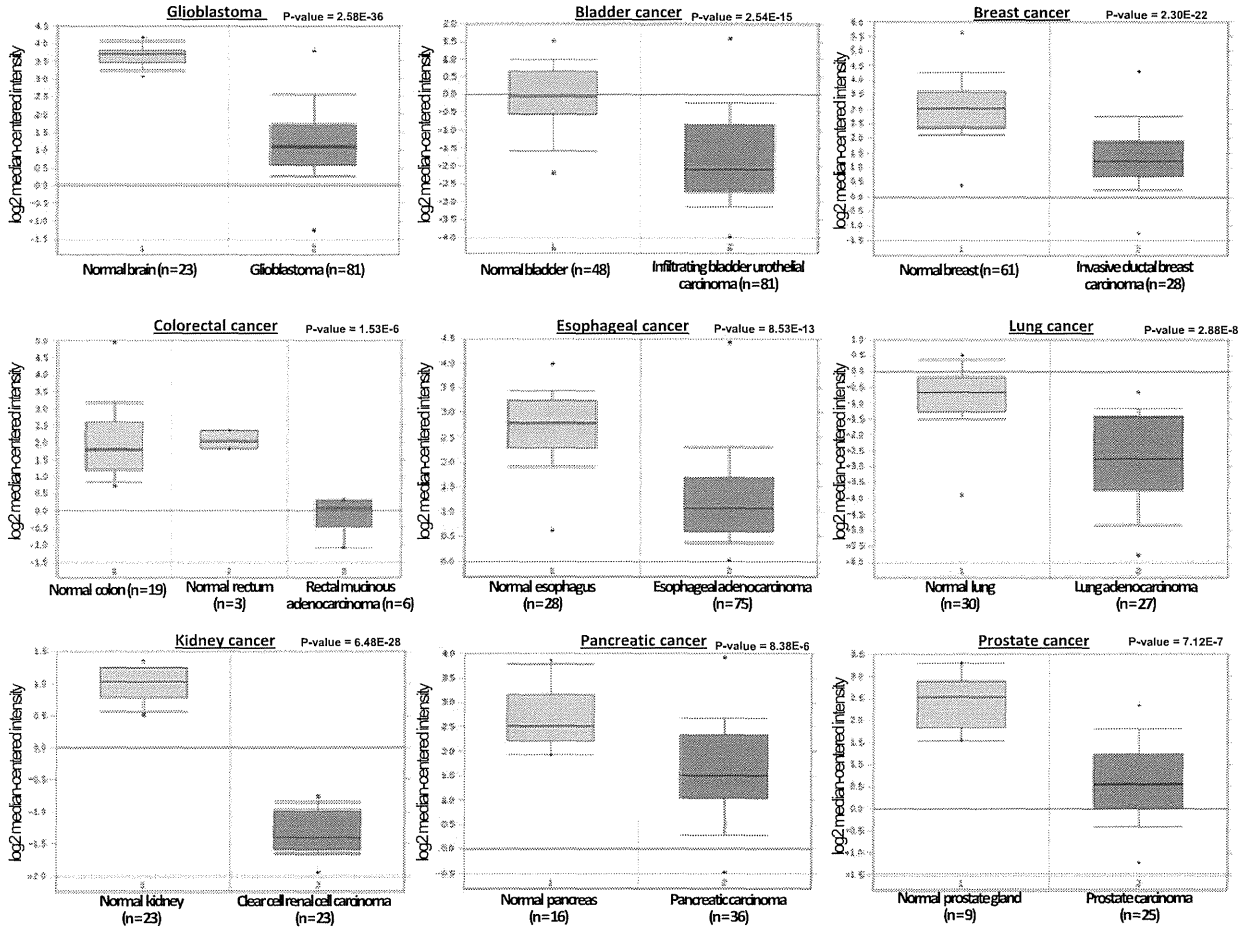

Figure W7. Expression of *GNAO1* in cancer tissues. Expression levels of *GNAO1* are downregulated in various types of cancer. Gene expression data in Oncomine were analyzed. The thick bars in the boxes are average expression levels, and the boxes represent 95% of the samples. The error bars are above or below the boxes, and the range of expression levels is enclosed by two dots.

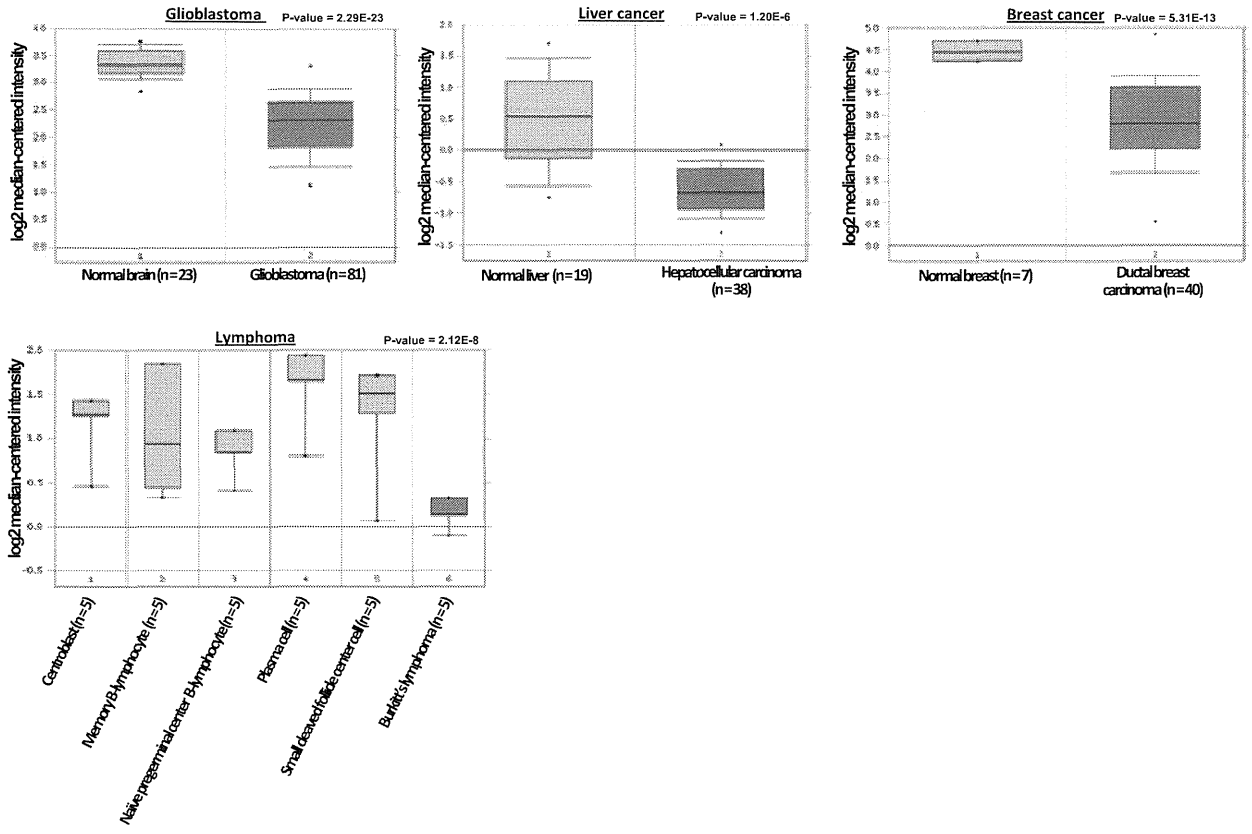

Figure W8. Expression of *ATG2B* in cancer tissues. Expression levels of *ATG2B* are downregulated in various types of cancer. Gene expression data in Oncomine were analyzed. The thick bars in the boxes are average expression levels, and the boxes represent 95% of the samples. The error bars are above or below the boxes, and the range of expression levels is enclosed by two dots.

Table W6. Comparison of H2BK120 Monomethylation and H3K27 Trimethylation Status in the Gene-Regulatory Regions of Downstream Candidates.

Gene Name	H2BK120me1*	H3K27me3*
KCNAB1	0.018	0.024
GNAO1	0.044	0.58435
ATG2B	0.04	NA†
MOV10	0.021	NA†

*Value is the ratio of tag number (siEZH2/siNC).
†NA; No significant methylation was detected in both siEZH2 and siNC samples.